Appendix

Contents

1. Null corrector ZEMAX design.

System/Prescription Data

File : C:\Program Files\ZEMAX\Samples\Lick null lens\lick null.ZMX
Title:
Date : MON AUG 6 2007

GENERAL LENS DATA:

Surfaces	:	16
Stop	:	8
System Aperture	:	Float By Stop Size = 1200
Glass Catalogs	:	SCHOTT
Ray Aiming	:	Paraxial Reference, Cache On
X Pupil shift	:	0
Y Pupil shift	:	0
Z Pupil shift	:	0
Apodization	:	Uniform, factor = 0.00000E+000
Effective Focal Length	:	37.73496 (in air at system temperature and pressure)
Effective Focal Length	:	37.73496 (in image space)
Back Focal Length	:	154.7869
Total Track	:	7647.153
Image Space F/#	:	0.8810274
Paraxial Working F/#	:	1.729532
Working F/#	:	1.978668
Image Space NA	:	0.2777229
Object Space NA	:	0.2682215
Stop Radius	:	-1200
Paraxial Image Height	:	0
Paraxial Magnification	:	0
Entrance Pupil Diameter	:	42.83063
Entrance Pupil Position	:	-44.30476
Exit Pupil Diameter	:	42.83063
Exit Pupil Position	:	74.10853
Field Type	:	Angle in degrees
Maximum Field	:	0
Primary Wave	:	0.6328
Lens Units	:	Millimeters
Angular Magnification	:	0

Fields : 1
Field Type: Angle in degrees

#	X-Value	Y-Value	Weight
1	0.000000	0.000000	1.000000

Vignetting Factors

#	VDX	VDY	VCX	VCY	VAN
1	0.000000	0.000000	0.000000	0.000000	0.000000

Wavelengths : 1
Units: µm

#	Value	Weight
1	0.632800	1.000000

SURFACE DATA SUMMARY:

Surf	Type	Comment	Radius	Thickness	Glass	Diameter	Conic
OBJ	STANDARD		Infinity	121.221		0	0
1	STANDARD	RELAY LENS	Infinity	18.77	BK7	61.16655	0
2	STANDARD	RELAY LENS	-52.475	163.5332		76	0
3	STANDARD	KPX630	Infinity	3.21	BK7	25.4	0
4	STANDARD	KPX630	-389.04	3		25.4	0
5	STANDARD	KPX621	233.424	3.35	BK7	25.4	0
6	STANDARD	KPX621	Infinity	136.8768		25.4	0
7	STANDARD		Infinity	7200		34.12903	0
STO	STANDARD	PM	-7200	-7200	MIRROR	2400	-1
9	STANDARD		Infinity	-136.8768		32.53763	0
10	STANDARD		Infinity	-3.35	BK7	13.1033	0
11	STANDARD		233.424	-3		13.81255	0
12	STANDARD		-389.04	-3.21	BK7	14.76948	0
13	STANDARD		Infinity	-163.5332		15.34919	0
14	STANDARD		-52.475	-18.77	BK7	64.46038	0
15	STANDARD		Infinity	-118.4133		61.85348	0
IMA	STANDARD		Infinity			0.001171664	0

SURFACE DATA DETAIL:

Surface OBJ	:	STANDARD
Surface 1	:	STANDARD RELAY LENS
Surface 2	:	STANDARD RELAY LENS
Aperture	:	Floating Aperture
Maximum Radius	:	38
Surface 3	:	STANDARD KPX630
Aperture	:	Floating Aperture
Maximum Radius	:	12.7
Surface 4	:	STANDARD KPX630

2. Hologram manufacturing test report.

Fabrication and Certification of High-Quality and Large - Aperture CGHs for Optical Testing

A. G. Poleshchuk, V. P. Korolkov

Institute of Automation and Electrometry SB RAS, Novosibirsk, 630090, Russia
e-mail: Poleshchuk@iae.nsk.su

Abstract: Laser-writing systems operated in polar coordinates and direct writing technologies for fabrication of large size (up to 300mm) and high precision (50nm) CGHs are described. Methods for certifying fabrication process are developed and experimentally validated.

OCIS codes: (050.1970) Diffractive optics, (220.4840), Optical testing

1. Introduction

One of the most promising trends in optical fabrication and testing is a wide application of computer-generated holograms (CGH) or diffractive optical elements. It is necessary to emphasize that many problems in optical testing can be solved only with CGHs application. Potential of CGHs is governed in many respects by the fabrication technology that must ensure the desired technical parameters.

In the present paper we consider the characteristic features of last version of specialized laser-writing systems (LWS) operated in polar coordinates [i,ii] used in fabrication of highly precise large CGHs. The problem of optimizing the writing strategy in order to reduce the errors is discussed. Methods for measuring and recording the writing process parameters during CGH fabrication, which allow one to estimate independently the error distribution for the element microstructure in the radial and angular coordinates are considered. The data recorded can be used for introducing corrections immediately during writing and also taken into consideration in further application of the CGH. In the paper we represent practical results on CGH fabricating obtained by means of LWSs located at the IA&E SB RAS (Novosibirsk, Russia).

2. Laser writing system operated in polar system of coordinate.

Fig. 1a shows a schematic layout of the LWS. The substrate with the recording layer is fixed on the 300mm face plate of the air bearing spindle. The angular encoder and frequency multiplier form clock pulses (~$3 \cdot 10^6$ per revolution) which are used to synchronize the laser writing beam modulation with the substrate rotation. The air bearing stage and the linear drive provide displacement of the optical writing head. The laser interferometer measures displacement of the stage with a resolution of about 0.6 nm. The accuracy of laser beam positioning is 50 nm. Two acousto-optic modulators (AOM) control the beam power (analog and binary modulation) of the argon laser in extended dynamic range. The writing head (including autofocus system, microscope with CCD camera, photodetectors and deflector) displaced vertically on air bearings and forms a 0.6 μm (FWHM) writing light spot. LWS operates in polar coordinate system and gives the possibility to write not only high quality rotationally-symmetric patterns, but also arbitrary ones (see Fig.1b and Fig.2b).

3. Methods of CGH fabrication.

The LWS allows us to fabricate CGHs with binary or continuous-relief microstructure onto large-diameter and thick optical substrates. The CGH patterns can be created using an exposure of photoresists and also a direct writing method based on thermochemical effect of laser heating on chromium films [iii]. Laser heating of chromium causes build-up of a thin oxide layer and microstructure change of the films, which considerably slows down liquid etching in etchants selective with respect to chromium oxides. This method permits the direct formation of chromium patterns with spatial resolution better than 1500 mm^{-1} without photoresist.

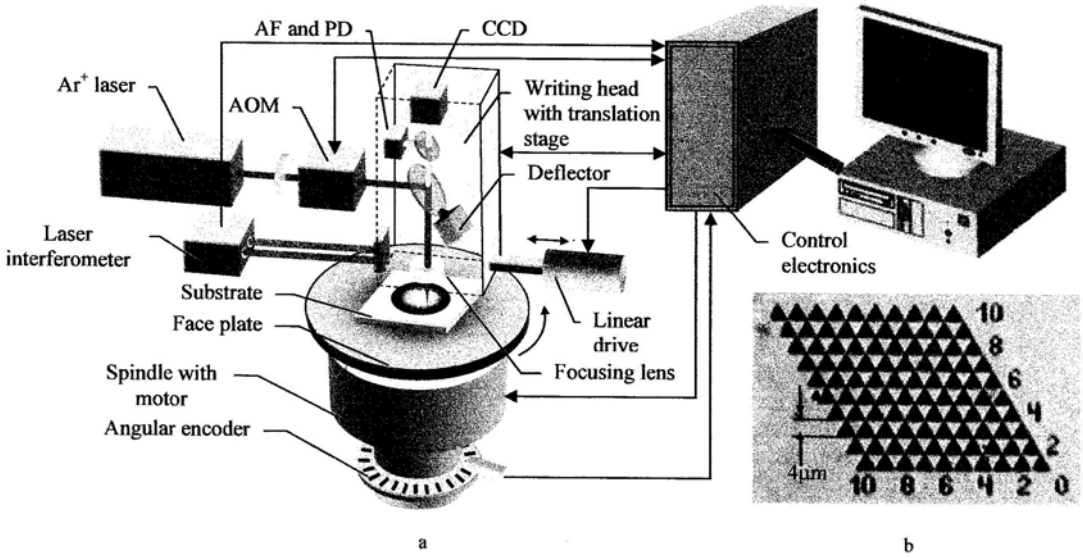

Fig.1. Schematic layout of the laser writing system (a) and test pattern written in chromium film (b).

The intensity of the laser beam is chosen to get given linewidth in range of 0.4-1.5 μm. After the pattern is exposed, it is developed by immersing the substrate in a caustic bath that dissolves the bare chromium much more quickly than the chromium oxide (see Fig.2a).

4. Specific sources of LWS errors.

The writing process introduces errors in CGH structure [2, iv, v]. These errors have two components: the difference between the calculated and real coordinates of diffractive zones in CGH, and the difference in shape between the calculated and actually fabricated zones. The absolute error of the coordinate depends on the accuracy of writing beam displacement with respect to the substrate rotation axis. Coordinate error results in an additional phase shift of the wavefront of the light flux transmitted through the fabricated CGH. The different writing errors of LWS were investigated. Some results are presented in Table 1.

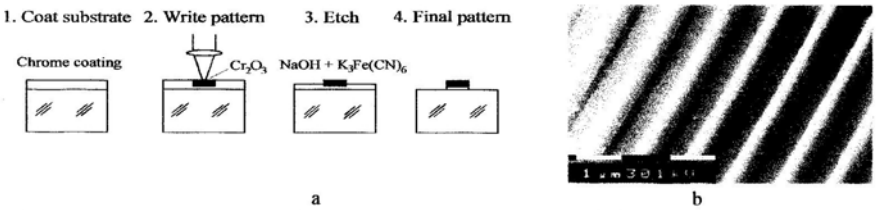

Fig.2. Pattern formation using thermochemical method (a) and fragment of CGH written in chromium film (b).

Table 1. Sources of LWS errors.

Error type	*Methods for error reduction*
The error of fixing the origin of coordinates	Accurate search of rotation axis
Drift of the origin of coordinates during writing	Periodical correction, prediction of CGH distortion
Error of circular shape of zones because of spindle runout	Real-time correction, prediction of CGH distortion
Errors of absolute radial coordinate of writing spot	System calibration, correction
Angular coordinate error	System calibration, correction

5. Strategy of CGH writing.

Writing strategy for non-axial-symmetric CGHs is very similar to typical step-by-step writing strategy for x-y writers. More interesting challenge is to get maximal fabrication accuracy for axial-symmetric CGHs [7] having wide application at the aspheric optics testing. Table 2 presents some peculiarities of such writing process realized in LWS at IA&E SB RAS. The majority of offered techniques results in an increase of writing time of DOE.

Table 2. Methods of writing.

Method	*Expected Result*
Circular step-by-step scanning	Less discretization errors
Multiple passes at writing of narrow diffractive zones	Uniform zone width change
Symmetric filling-in of the zones	Uniform zone width change
Scattering of the start points of circular trajectories in angular sector	Angular uniformity of the pattern

6. Certification of CGH.

Since the aspherical surfaces are fabricated using the results of the test, the null CGHs define the shapes of the final optics. But there is always a possibility that the null CGH could be flawed, resulting in final shape of the optics being incorrect. Problem is that the aspherical wavefront generating by CGH cannot be tested by standard methods. Several methods of indirect CGH certification have been developed [vi, vii,viii]:

- Preliminary calibration of LWS and systematic inaccuracy compensation.
- Periodical correction of LWS errors during writing process.
- Measurement of current errors of LWS during writing and then using data *to* calibrate optical test systems.
- Embedding special fiducial reference marks and zones in CGH.
- Writing the test zone plates and their testing before fabrication of CGH.
- Sub-aperture combining a test zone plate and the CGH on one substrate.
- Fabrication diffractive imitator of the tested surface.

7. Conclusion

We have designed and built a high precision polar coordinate LWS. This system can produce arbitrary (not only rotationally symmetric) CGHs on large (300 mm) substrates. Resistless technology for writing on chromium films has been developed. CGHs and test structures were presented to demonstrate that this device is an extremely useful tool for CGH fabrication.

Certification of fabrication process by means of preliminary writing a ruler composed from special fiducial marks is new powerful way to confirm the accuracy of CGH. The developed writing technologies have been demonstrated with fabrication of the large number CGHs with diameter of up to 220mm [ix] for optical testing and have shown that the wavefront error does not exceed 0.01λ rms corresponding to a 50 nm pattern accuracy.

References

i. A.G. Poleshchuk, E.G. Churin, V.P. Koronkevich, V. P. Korolkov, etc., "Polar coordinate laser pattern generator for fabrication of diffractive optical elements with arbitrary structure," Appl. Opt., **38**, 1295-1301 (1999).

ii. A.G. Poleshchuk , V. P Korolkov, V. V Cherkashin., S. Reichelt, J.H. Burge. "Polar coordinate laser writing system: error analysis of fabricated DOEs," SPIE **4440**, 161-172 (2001).

iii. V. V. Cherkashin, E. G. Churin, V. P. Korolkov, V. P. Kooronkevich, A. A. Kharissov, A. G. Poleshchuk, J. H. Burge, "Processing parameters optimisation for thermochemical writing of DOEs on chromium films," SPIE. **3010**, 168-179 (1997).

iv. V. V. Cherkashin, A. A. Kharissov, V. P.Korol'Kov, V. P. Koronkevich, A. G. Poleshchuk, "Accuracy potential of circular laser writing of DOEs," SPIE **3348**, 58-68 (1998).

v. A.G. Poleshchuk, V.P. Korolkov, V.V. Cherkashin, S. Reichelt, J.H. Burge. "Methods for minimizing the errors in direct laser writing of diffractive optical elements," Optoelectr., Instrum. and Data Process., **38**, No. 3, 3-13 (2002).

vi. A. G. Poleshchuk, V.P. Korolkov, V.V. Cherkashin, J. Burge."Methods for certification of CGH fabrication," Trends in Optics and Photonics, (OSA Topical Meeting "DOMO-2002", June 3-6, 2002, Tucson, USA). **75**, 438-440 (2002).

vii. R.K. Nasyrov, A.G. Poleshchuk, V.P. Korolkov, K. Pruss, S. Reichelt. "Certification of diffractive optical elements for aspherical optics testing," Optoelectr., Instrum. and Data Process. **41** No. 1, 100-108 (2005).

viii. J.-M. Asfour, A. G. Poleshchuk. Asphere testing with a Fizeau interferometer based on a combined computer-generated hologram," JOSA A, **23**, Issue 1, 172-178 (2006).

ix. J.H. Burge, V.V. Cherkashin, V.P. Koronkevich, A.G. Poleshchuk. "Measurement of 6.5 and 8.4-meters aspherical mirrors shape by computer generated holograms," Proc. of IV Intern. Conf. on Applied Optics (Oct. 18-22, 2004., St.-Petersburg), **III**, 203-207 (2004).

REPORT

ROC-PM2 Computer Generated Hologram Manufacturing

Hologram patterns were designed and specified in detail by Dr., Prof. **Jim H. Burge** (Tucson, AZ, USA).

REQUIREMENTS

The requirements for manufacturing holograms as a pattern of chrome rings on a bare glass substrate are:

- hologram distortion (μm scale) 0.3
- hologram distortion (μm rms) 0.04
- substrate figure (rms waves) 0.005
- chrome thickness variation (nm rms) 2
- hologram pattern defined using the supplied files
- accuracy of aligning hologram and pattern <0.05mm

1. Substrates.

Table 1. Hologram substrate.

	ROC-PM2
Material of substrates	fused silica
Diameter, mm	50
Thickness,	5
Surface flatness over 35 mm field (P-V/rms)	0.04/0.01
Coating	~70-80nm Cr-film

Results of the substrates testing are shown in Fig.1.

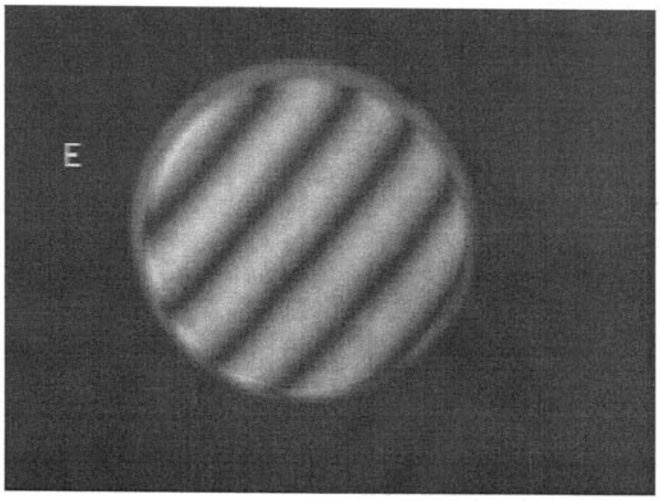

Fig. 1. Interferograms of 50 mm substrate coated with 70nm chromium film for ***ROC-PM2*** hologram.

2. Hologram composition

Table 2

	ROC-PM2
Rings for centering R_{min}, R_{max}, μm	0 – 35
Zone plate structure, R_{min}, R_{max}, mm	0.03-17.2
Data filename:	ROC-PM2.DAT
1 μm test ring, R, mm	17800
Caption (Hologram: ROC-PM2. #02; Test ring 17800um; T=18.4C; P=1022; CLWS300 IA&E 16/01/04), mm	19-20.5
Mark (1x1mm) for computing origin	Yes
Writing laser power tests, R, mm	19
Ruler	Yes

3. Writing errors.

3.1 Writing conditions and displacement errors.

Laser interferometer's wavelength (in vacuum) is 632.990989 nm (tested by Iodine sell).

Table 3

	ROC-PM2
Temperature	*18.5±0.05 C°*
Air pressure	*1022 mbar*

Laser writing beam displacement error (0-8mm hologram radius) is no more 0.05 μm (p-v) and 0.01μm (rms).

3.2. The errors of fixing the origin of coordinate.

Coordinates of hologram center (origin of coordinate) are measured before, during and then after finishing hologram pattern writing. Measured data of center errors (error of origin of polar coordinate) in the time of ROC-PM2 holograms writing are given in Table 4. Center error ε_r corresponds to CGH pattern distortions at given radius r.

Table 4

Measurements of center errors, R, mm	*ROC-PM2, ε_r, μm*
17.1 (start of writing)	-0.009
16	-0.048
14	-0.031
12	-0.014
10	0.026
8	-0.009
6	0.01
4	0.016
2	0.056
0 (end of writing)	0.015
RMS error	**0.03**

Thus, peak coordinate error between start and end of holograms writing is not exceed of 0.018 μm.

Wavefront errors produced by CGH pattern distortions can be calculated as:

$$W_r = \lambda \cdot \varepsilon_r / S$$

where: ε_r - CGH pattern position error, S - localized CGH pattern spacing.

3.3 Trajectory of rotation.

Trajectory of spindle rotation was defined before writing process by means of measurement of many diameters of small test ring (~50 μm diameter). Measured deviation of the trajectory of spinning table rotation from an ideal circle is shown in Fig. 2. Deviation of the trajectory of rotation (and, hence, shape of hologram zones) is no more ±0.04μm.

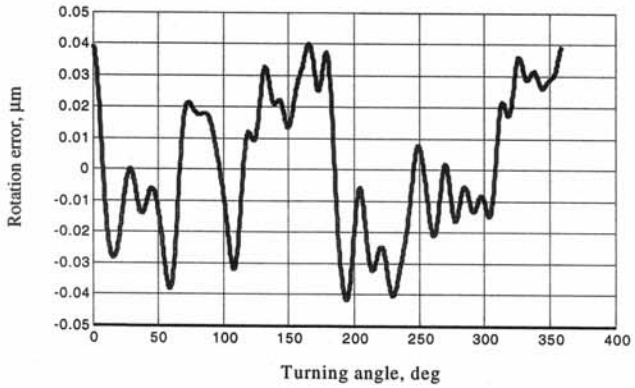

Fig. 2. Trajectory of spindle rotation (with correction). Deviations are no more ±0.04μm (>0.02μm rms). Inaccuracy of measurement is about 0.01μm (rms).

4. Independent certification of hologram pattern.

4.1 Ruler

To certificate the hologram pattern a special small marks are used. These marks are written directly before of the main hologram pattern writing. Every mark consists of small parts of hologram pattern (~10 x10 μm). Time of the some marks writing is a few seconds (typically about 10-20 s) and writing errors are practically absent. For convenience of mark observation they are written along hologram radius as shown in Figure 3 and form a ruler. Value of the ROC-PM2 ruler scale division is 2 mm.

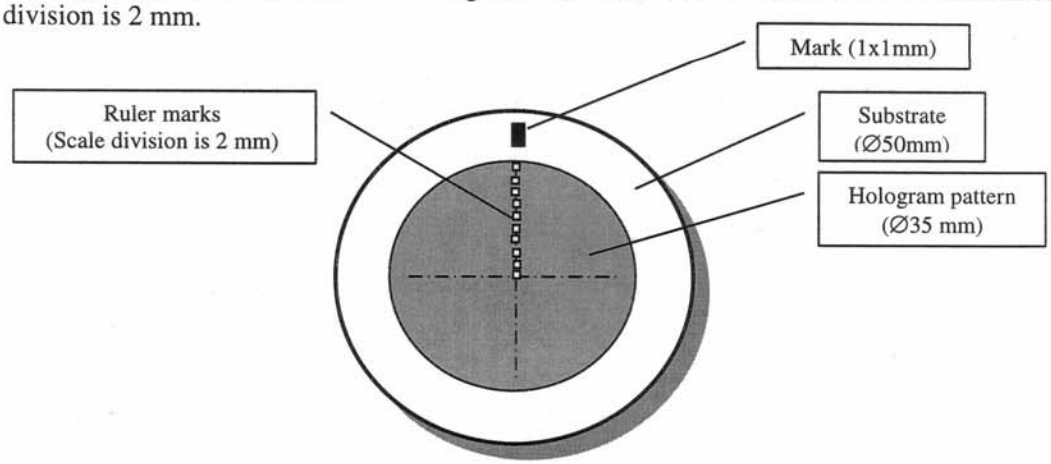

Fig. 3. Ruler location.

Shift of ruler lines (in marks) relatively to hologram pattern (zones) is equal to writing error at corresponding radius. Results of measurements are presented in Fig. 4 and Table 5. Writing errors are within accuracy of measurements.

4

Table 5

Graduation marks:	Shift of ruler lines, μm (p-v) ***ROC-PM2***
At R=5mm	<0.1
At R=4mm	<0.1
At R=3mm	<0.1
At R=2mm	<0.1
At R=1mm	<0.1

* Accuracy of the measurements is about ±0.05μm

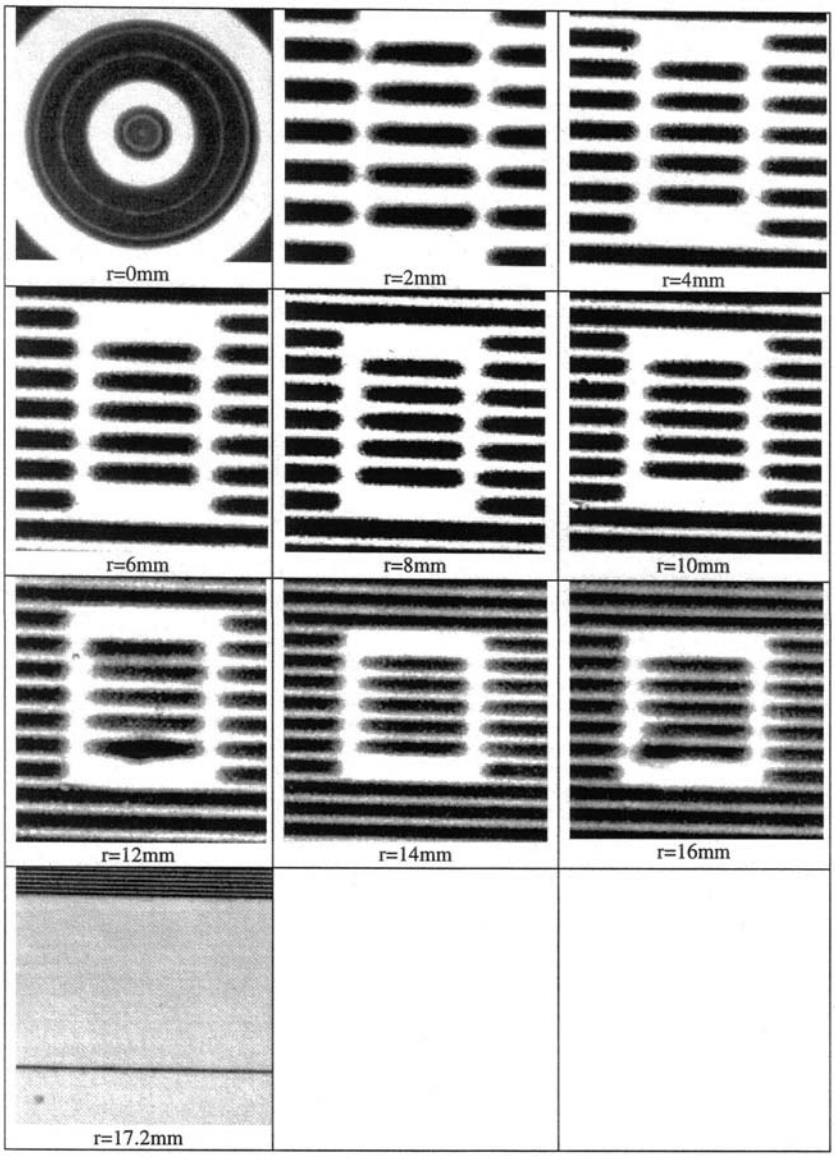

Fig 4. Microphotographs of center, ruler graduation marks and control ring of ROC-PM2 hologram

5. Error summary.

Table 6. Error summary for **ROC-PM2** holograms fabrication.

Error term (Manufacturing errors)	*Value (rms), δ_{rms}*
	ROC-PM2#02
Substrate flatness, λ	0.01
Radial coordinate (writing error), μm	0.01
Origin of coordinates, μm	0.03
Trajectory of rotation, μm	0.02
Data representation, μm	0.001
Chromium film thickness variation along hologram, nm	<2

We certify that the **ROC-PM2** holograms (sample #02) meets the requirements.

Lick 2.4 m Primary Test Plan

1. Null lens calibration.

1.1. Test description.

Calibration of the null lens is critical in the determination of the mirror's surface figure quality since any error in the null lens results in an error in figuring the mirror. If the mirror is figured perfectly to an imperfect null lens the mirror will contain errors mirroring the null lens errors: the now classic "Hubble" error. The null lens is designed to eliminate the spherical aberration of the primary tested from its center of curvature when tested with the mirror having the correct design values of radius and conic constant. Incorrect mirror parameters will cause errors in the null lens measurement as well, due not to the null lens but to the incorrect parameters. These errors will be evaluated separately and the final data corrected.

The first problem is to correctly calibrate the null lens so that its errors are known and can be considered in the measurement process either subtracting them from the test data or, if small, adding them to the final estimate of the figure error as part of the error budget. Calibration begins with a good design for the null lens that is shown in Figure 1. The design is an Offner type with the field lens comprised of two lenses. An earlier design having a single field lens resulted in a null lens that produced a bad ghost image and splitting the lens using two plano-convex lenses completely eliminated any ghost reflections except inside the central obscuration. This design has a residual wavefront error of 6.8 nm rms.

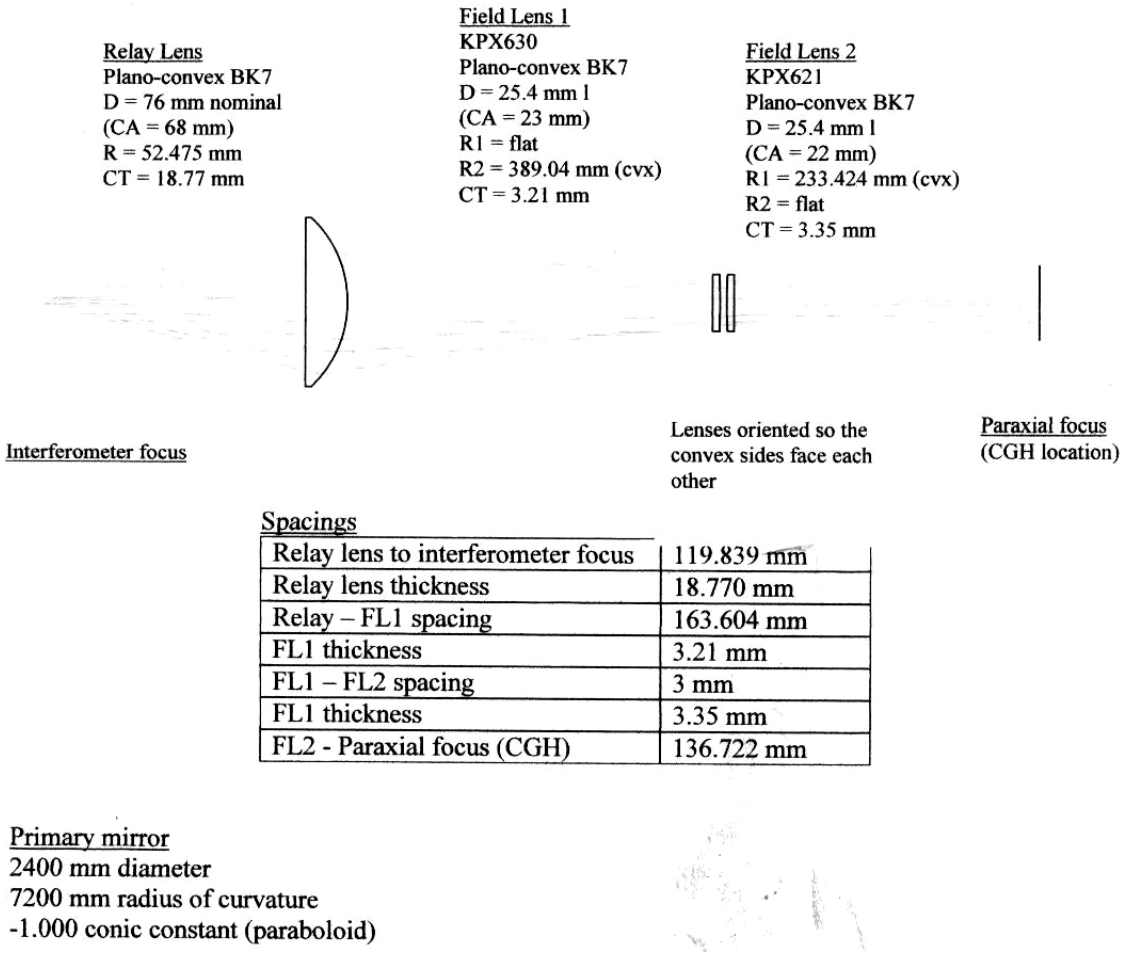

Figure 1. The Offner null lens design for the primary mirror.

The lenses were fabricated to high quality and installed in a special cell mounted on a 3-axis stage in front of the interferometer as shown in Figure 2. Final alignment and calibration of the lens is performed using a computer-generated hologram designed to be placed at the paraxial focus of the null lens. An ideal CGH would return a wavefront that matches that of a perfect primary mirror. Any measured errors in the wavefront would be due to limitations in the null lens. These errors can then be calibrated out of the data from the mirror measurement. As the CGH is not perfect, errors in the CGH will then limit the accuracy of the final test. These errors are much smaller than the errors from the null lens. The parameters for the CGH are shown in Table 1 and a summary of the analysis of the CGH accuracy is shown in Table 2. The analysis shows that the uncertainty in the mirror's surface figure due to the CGH calibration is 6.2 nm rms.

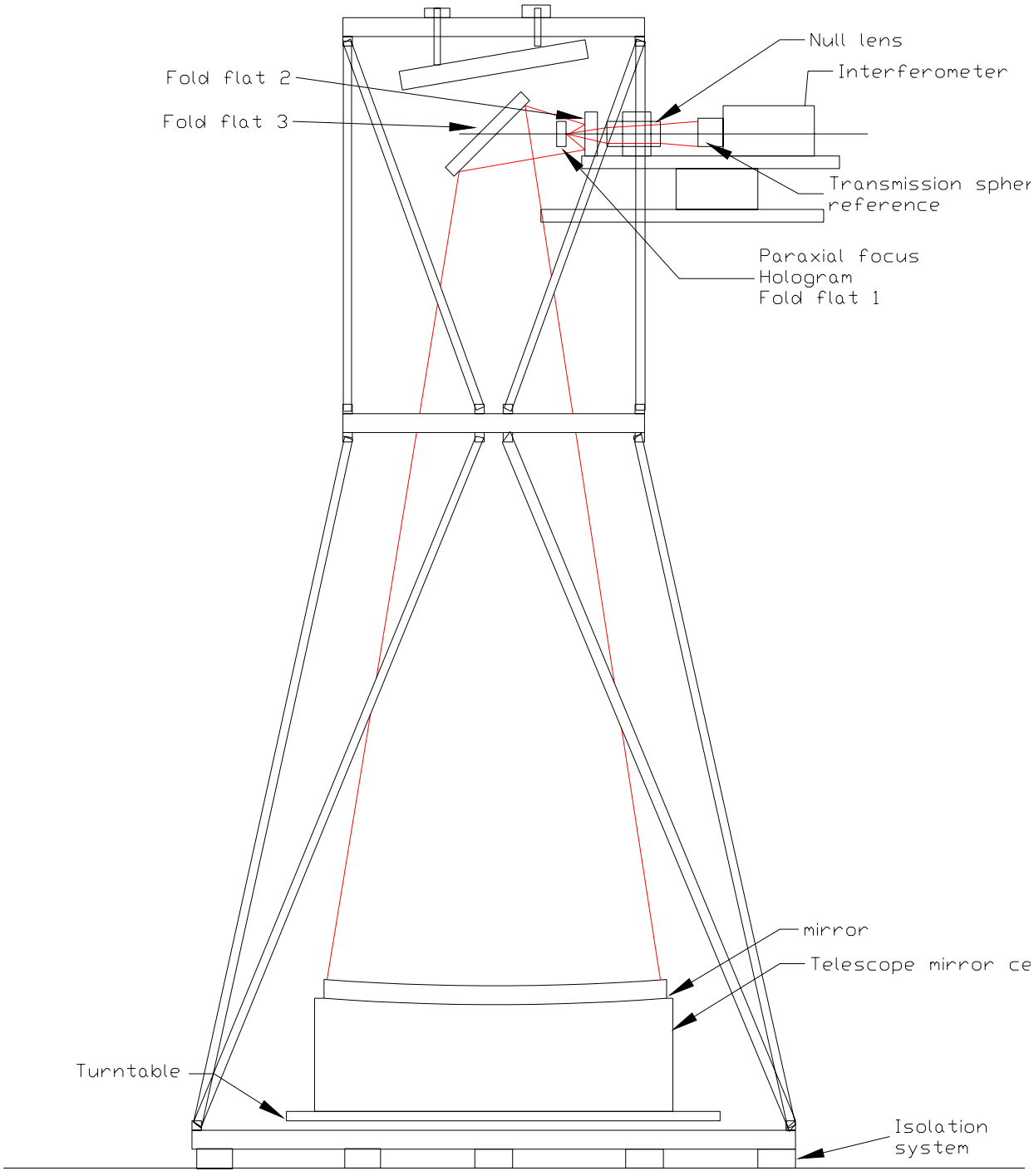

Figure 2. General schematic of the primary mirror test setup in the 8-m tower.

CGH type	Chrome on glass
Filename with parameters	ROC-PM2.H
Duty Cycle	50%
Number of rings	7082
Outside ring radius	17.730 mm
Outside ring width	0.94 µm
Substrate flatness	< 0.006 wave rms over clear aperture
Pattern scale error	< 0.5 µm/radius
Pattern distortion	< 0.040 µm rms

Table 1. The design parameters for the CGH.

			in waves	
Error term		**dK (ppm)**	**SA p-v**	**figure rms**
hologram distortion (µm scale)	0.5	60	0.016	
hologram distortion (µm rms)	0.04			0.0070
substrate figure (rms waves)	0.006			0.0060
chrome thickness variation (nm rms)	2			0.0032
root sum squared		**60**	**0.016**	**0.0098**
equivalent nm rms			**3.1**	**6.2**

Table 2. The estimated errors due to the CGH.

1.2. Calibration procedure.

The procedure we use to perform an *in-situ* calibration of the null lens with the CGH is as follows:

1. **Make sure the mirror is covered before performing this calibration.**

2. Unscrew the retaining ring at the rear of the fold flat #1 mount and carefully remove the fold flat.

3. Carefully insert the hologram into the mount with the hologram facing the null lens. The hologram's rear surface has been marked with 8 marks 45 degrees apart to allow for orienting the hologram in the test. Rotate the hologram so that it's 0 deg mark is lined up with the mount's index mark that is scribed at the top rear surface of the mount.. Replace the retaining ring and tighten just to very lightly touch the hologram. Back the ring off about 1/12 turn.

4. Loosen the bolt at the base of the mount and rotate the mount so that it is perpendicular to the null lens axis. The paraxial focus of the null lens should be very close to the center of the hologram.

5. Adjust the hologram in tilt and decenter to null the fringes from the hologram.

6. Adjust the source position and the null lens position to produce the smallest irregularity in the fringes as possible.

7. Load a full aperture phase map from a previous measurement of the primary mirror into memory.

8. Move the mask until it is centered on the nulled hologram interferogram.

9. Calibrate the phase shifter voltages using the procedure described in the Intelliwave manual for "Calibration of Phase-shifting Device". The software will automatically calibrate the voltages.

10. Measure the hologram with a wedge of .5 that will produce the same map scale as will the measurement of the primary mirror's surface error. (not wavefront). Measure 4 times and store each map with the file names **nullcal01, nullcall02, etc.**

11. Rotate the hologram 45 degrees lining up the next mark with the mount mark.

12. Repeat the measurement of the hologram after nulling the fringes **(do not move the null lens or source, only the hologram)**. Measure 4 times and store each map with the file names **nullcal451, nullcal452, etc.**

13. Rotate the hologram to the remaining 6 positions and remeasure each 4 times giving the file names **nullcal(angle)(measurement).** At the end of the process there should be 8x4 or 32 phase maps of the hologram.

14. Average the 32 maps. Observe each map before adding to the average to be sure the errors all have the sign of the wedge correct i.e., that the highs are high and the lows low. If they are not simply invert the map and restore it under the same file name.

15. The resulting phase map is the calibrated average of the null lens. Fit the map to the standard U of A set of Zernike polynomials. Subtract the two third order coma terms. (Tilt and focus have already been subtracted.)

16. Fit the resulting data to the high order Perkin-Elmer set of Zernike polynomials. Do not subtract anything using this set.

17. Store the resulting map using the file name **lick null (date).** For example, if the data was taken on September 12, 2006 name the file **lick null 091206.**

18. This map defines the test optic errors due to the null lens and reference surface. The same mask must be used for all subsequent tests of the mirror. If the mask is changed in size (except by scaling) this calibration must be repeated. See the test description of the mirror for the method of subtracting this data. The null lens and source must not be adjusted for this test to be valid.

2. Phase-measurement of the mirror's surface errors.

2.1 Test description.

Shown in Figure 2 is a schematic of the test depicting the principal components. The primary mirror is being final figured and tested while mounted in the actual telescope cell provided by EOST. The mirror is supported axially at 27 points on invar pads that have been bonded to the surface. The only lateral restraint is through the thin flexure plate holding the mirror laterally at three points near the center hole. No other forces during testing are exerted on the mirror. The cell is clamped to the machine turntable at three of the "feet" at the bottom of the cell. After considerable polishing in this condition the mirror has shown no motion and we consider the system to be very stable.

Supported on a platform above the mirror near its center of curvature is the interferometer/null lens assembly. Because of the proximity of the system to the large, unused fold flat that resides at the top of the tower the beam has to be folded with three flats to direct the beam down to the mirror. These flats are of 2", 4" and 16" apertures. Although they are each of high quality, $\lambda/20$ p-v or better, they are used double pass in the test and can be expected to introduce some asymmetric error into the test. We assume that the symmetric errors other than power will be very small. The spherical aberration error will be estimated from the independent tests of the flats and folded into the final test results. The asymmetric errors will be evaluated and removed through multiple mirror rotations. The null lens errors will be evaluated separately and subtracted (see section 1.1).

Intelliwave software will be used for the phase-measurement of the mirror, the same as was done for the null lens calibration. The same algorithm used for the null lens cannot be used for the mirror measurement since the vibration level of the mirror is currently large enough to preclude the phase-stepping type of algorithm, although we are working on ways to improve this. Instead, we will use Intelliwave's single frame algorithm that calculates the phase with the use of a spatial carrier introduced by putting a specific amount of tilt into the interferogram to assure a 90-degree phase shift pixel to pixel across the pupil. Due to the fact that some tilt must be introduced into the test to provide the spatial carrier the test is not strictly common-path passing through the system. Some asymmetric errors, though small, can arise due to the fact that the beam is not traveling through the null lens quite on axis. This problem is completely nulled when measurements are made with equal and opposite signs of tilt and the two results averaged together. This eliminates the asymmetric error arising from the tilt, typically some small amounts of high-order coma and astigmatism. Third-order coma, the largest component, is an alignment error in the test and is subtracted from the measurements directly. The amount of coma in the mirror is related to the amount of decenter in the optical axis and will be evaluated as described in Section 3.

2.2. Test procedure.

1. Align the mirror rotationally to the 0 degree mark on the turntable.

2. Place fiducial set on the mirror surface.

3. Load the null lens reference file **lick null (date).**

4. Align the pupil mask to the pupil image in the interferometer.

5. Check that the following switches have been set:

    a. Measurement method: static fringe, horizontal tilt (fringes vertical).
    b. Wedge of .5 (surface values)
    c. No smoothing of interferogram
    d. No clipping of data
    e. 3x3 median smooth of OPD
    f. No spike clipping
    g. No automatic OPD calculation
    h. Tilt and focus removed 36 term UofA Zernike fit.
    i. Reference subtract on. (Null lens calibration subtracted.)
    j. Minimum discontinuity method of unwrapping. (Slow, but high quality)

6. Align the fiducials on the mask with the real surface fiducials.

7. Set the four target fiducials.

8. Switch to Reference mode and align the reference map to the current mask position by using the “translate reference” interactive menu.

9. Switch video mode to view wrapped fringes.

10. Align the horizontal tilt to null the wrapped fringes. Note in the notebook the time, orientation of the mirror, the room temperature, and the direction of tilt. Assign file name.

11. Take a set of 5 interferograms. Check that the modulation is above .15 and that the average phase is above 80 degrees. Visually select a clear interferogram from the five and select “compute OPD”.

12. Inspect the resulting phase map for continuity and obvious errors. Check that the wedge has the correct sign (through previous measurements of the surface). The subtraction of

the reference data set should not clip the pupil. If it does go back and realign the reference data set. If the map looks smooth and continuous then fit the data to the 36 term Uof A Zernike set.

13. Select and subtract the two third order coma coefficients.

14. Store the resulting data under the assigned file name keeping time-ordered numerical count of the phase maps.

15. Repeat steps 9-13 measuring the mirror a total of 15 times.

16. Go back to video mode and tilt the fringes horizontally to the other side of the wedge and null the fringes. The switch "invert pupil" must be turned on or off to switch the sign of the wedge so the phase map has the correct sign. Make sure that the reference and the pupil mask match.

17. Repeat steps 9-13 measuring the mirror a total of 10 times.

18. Rotate the mirror 90 degrees clockwise so the mark on the turntable labeled "90" lines up with the reference mark.

19. Realign the mask with the fringes. If the mask was translated, the reference will need to be realigned with the current mask.

20. Null the fringes and reset the "target" fiducials.

21. Switch the video to wrapped phase mode and null the fringes by adjusting the tilt and focus of the interferometer.

22. Repeat steps 9-13 measuring the mirror a total of 15 times. Note in the notebook the time, orientation, and direction of tilt. Assign a file name with "90" for the orientation.

23. Repeat steps 16-17 measuring the mirror a total of 15 times.

24. Repeat steps 18-23 after rotating the mirror to the "180" position.

25. Repeat steps 18-23 after rotating the mirror to the "270" position.

26. Average the results of the four sets of data from each of the 4 mirror orientations and store the result with the file name including the orientation. Record the file names in the notebook.

27. Check that each of the averaged files has the same sign of the wedge. If not invert as necessary and restore the data.

28. Check that each of the data files shares the same mask with the mask in the identical location as the mirror at the initial "0" degree location. Load and translate the maps as necessary to align the maps so they all share the identical map position. Resave the translated maps and record the final file names in the notebook.

29. Average the four data sets and save. Record the file name in the notebook.

30. Fit the data to the 36 term UofA Zernike data set.

31. Subtract all of the symmetric terms as well as the third order coma terms.

32. Use the theoretical data interactive menus to generate a phase map of the remaining asymmetric Zernike terms. Save the map and record in the notebook. This map represents the non-rotationally symmetric component of the test-optic errors due to the three fold flats.

33. Load the map from step 32 into the reference. Load the four test position averages one at a time into surface and subtract the reference. This subtracts the test optic errors from each of the tests. Make sure that there is no translation error between the surface and reference. Translate the reference as required. Save each final map with its angle and note the names in the notebook.

34. Using the final 0 position map as the target, use the fiducial transformation process to rotate each of the final phase maps to the 0 degree position. These 4 measurements should appear nearly identical under perfect measurement conditions. The 4 maps can be averaged to produce a final "best estimate" phase map of the surface.

35. The rms residuals value from the average must be root-sum-squared with the remaining uncertainties of the measurement. These are given in the table below.

Error source	Surface rms
Mirror surface residuals	TBD
Symmetric error of flat 1	2nm
Symmetric error of flat 2	3 nm
Symmetric error of flat 3	6 nm
Hologram errors	6.2 nm (wavefront) 3.1 nm surface

36. Using the values given in the above table calculate the final rms surface error. Multiply this value by 2 to give the rms wavefront error.

3. Measurement of the centration of the optical axis.

3.1. Introduction

When the optical axis of an aspheric mirror is decentered with respect to its mechanical center, small asymmetric errors will be present in the mirror's surface described by low order Zernike polynomials. After tilt, coma is the next largest aberration for small decentrations. If the coma present in the surface can be measured then the amount and direction of axial decenter can be computed from the magnitude and orientation of the coma.

Because coma also results from a misalignment of the null lens axis to the mirror's axis during an optical test it is required to rotate the mirror and perform two optical tests to separate the two sources of coma. It is essential that during the two tests the mirror's axis and the null lens's axis do not change with respect to one another. To accomplish this the null lens is not moved between the two tests except for some small focus (z) motion parallel to the optical axis that will not affect the measurement.

In the first test the coma is roughly minimize, i.e., the coma in the mirror is balanced by a tilt of the null lens axis. The fringes are nulled and measurements are taken retaining the coma terms. The mirror is then rotated 180 degrees and returned to the exact same position it had during the first test. This is done by carefully aligning the mirror's optical surface to the axis of rotation of the test tower turntable. Four dial indicators are placed 90 degrees apart at the top edge of the mirror for centration and on the mirror's surface for tilt. Adjustments are made in tilt and decenter of the turntable support plate to bring the indicators to a near null readout as the mirror is rotated.

The coma that is observed in the second test is related to the amount of coma in the mirror's surface giving a measure of the position of the optical axis. In the following analysis

$(a_3^{1,-1})_{T1}$ = the Zernike coma coefficients from the first test (mirror at 0 degrees)

$(a_3^{1,-1})_{T2}$ = the Zernike coma coefficients from the second test (mirror at 180 degrees).

$(a_3^{1,-1})_{M}$ = the Zernike coma coefficients of the coma present in the mirror's surface.

$(a_3^{1,-1})_{TO}$ = the Zernike coma coefficients of the test optics (not misalignment)

$(a_3^{1,-1})_{a}$ = the Zernike coma coefficients due to misalignment in the first test.

$(a_3^{1,-1})_{d}$ = the Zernike coma coefficients due to decenter of the mirror in the second test relative to the first test (as measured by the dial indicators).

Given these definitions

$$(a_3^{1,-1})_{T1} = (a_3^{1,-1})_M + (a_3^{1,-1})_{TO} + (a_3^{1,-1})_a$$

$$(a_3^{1,-1})_{T2} = -(a_3^{1,-1})_M + (a_3^{1,-1})_{TO} + (a_3^{1,-1})_a + (a_3^{1,-1})_d$$

then,

$$(a_3^{1,-1})_M = ((a_3^{1,-1})_{T1} - (a_3^{1,-1})_{T2} + (a_3^{1,-1})_d)/2$$

It can be shown that the amount of coma is related to the amount of decenter through the following relations:

$$(a_3^{1})_M = Kr^3x/6R^3$$

$$(a_3^{-1})_M = Kr^3y/6R^3$$

where x and y are the amounts of decenter of the optical axis, r is the aperture radius, K is the conic constant, and R is the radius of curvature.

For this mirror, given the requirement that the amount of decenter be less than 2 mm, the maximum amount of coma that is allowable in the mirror's surface is 3 microns P-V or just under 5 waves. This means that given a near coma null for the first test we should observe less than 10 waves of surface coma upon rotation of the mirror to the 180 degree position.

3.2. Procedure.

1. Place a double layer of electrical tape at the top edge of the mirror so that it folds over onto the optical surface. Make sure the tape remains smooth. Go around exactly twice with no triple overlap.

2. Set up 4 dial indicators around the mirror's edge, two pairs 90 degrees apart. The first pair should measure the lateral runout and the second pair should measure the tilt. The tilt indicators must only contact the tape and not the optical surface.

3. Adjust the tilt and centration of the turntable until the TIR on all indicators is less than .005".

4. Rotate the mirror until it is at the 0-degree location.

5. Prepare the mirror for optical testing. Note the location and values of the dial indicators in the notebook.

6. Place two additional fiducials on the mirror that locate the +y and +x directions in the measurement plane. Mark these locations in the pupil with small circular masks.

7. Test the mirror according to the procedure described in Steps 1-14 of "Phase-measuring of the mirror's surface figure except **do not remove the coma terms.**

8. Rotate the mirror to the 180-degree position and translate the interferometer to properly align the fringes. **Do not use the null lens tilt controls, as this will nullify the test.**

9. Test the mirror again as described in step 6.

10. Note the values of the dial indicators and record them in the notebook.

11. Load the 0-degree map into surface and fit to 36 term Zernikes (UofA). Note the two third order coma coefficients in the notebook.

12. Load the 180-degree map into surface and fit to 36 term Zernikes (UofA)

13. Using the coma coefficients and the relations described in the introduction compute the x and y coordinates of the axis decenter and record in the notebook.

14. Using the relation: arc tan $\theta = (a_3^{-1})_M / (a_3^{1})_M$ compute θ and record in the notebook. 0 degrees is along the +x axis established by the fiducials.

4. Measurement of the radius of curvature.

4.1. Introduction.

Shown above in Figure 2 is a schematic of the test setup used for optical testing as well as the measurement of the radius of curvature. Because the mirror is aspheric the radius of curvature varies with aperture radius so what we want to measure is the paraxial radius of curvature specified in the design. The distance to be measured is that between the mirror's surface and the paraxial focus. Locating the paraxial focus can be difficult but fortunately we can use the null lens calibration CGH to locate it very precisely because the CGH is designed to be placed at the paraxial focus of the null lens to null the wavefront. When the fringes are nulled in the test of the mirror the paraxial focus of the mirror will coincide with this point. If we locate the hologram plane during CGH testing, then remove it and insert and tilt fold flat 1 so that its axial position is unchanged, then the flat's position accurately locates the paraxial focus.

To accomplish this the hologram and fold flat 1 are both held in a gimbal mount that tilts the surface of the flat or hologram about the center of its surface. This mount is supported on a 3-axis stage that allows for translation of the flat laterally without changing the position axially. When the hologram is placed in the mount and the fringes from the null lens are nulled this accurately locates the paraxial focus. The hologram is then removed from the test and fold flat 1 is inserted into the mount so that its surface is coincident with the hologram plane. The flat is then pivoted about the gimbaled pivot to fold the beam onto the test beam path. The paraxial focus of the mirror is then located on the surface of the fold flat when the fringes from the mirror are nulled.

Because there are three fold flats in the beam there are three distances that must be measured that sum to the radius of the mirror. Figure 3 depicts the three fold flats looking down from the top showing two of the distances: the first between fold flat 1 and fold flat 2 and the second between fold flat 2 and fold flat 3. The third distance is that between fold flat 3 and the primary mirror's surface.

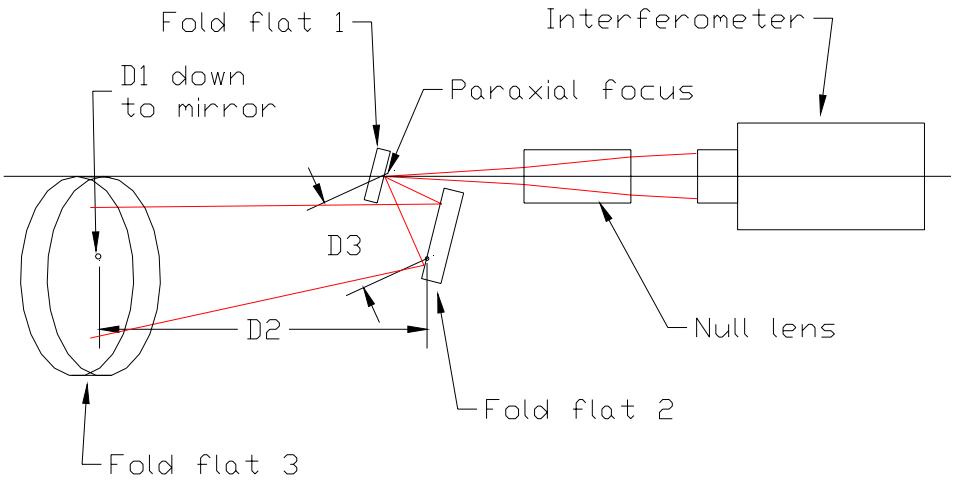

Figure 3. Top view of the test setup showing the fold flat arrangement.

Because the flats are tilted locations on the flats must be marked that follow a single ray from the primary to the paraxial focus. This is done by placing a small mark first on flat 3 while observing the fringes that marks a point in the pupil near the center of the mirror. A second mark is placed on fold flat 2 that coincides with the mark on flat 3. This is done by simply observing the image of the pupil and making the two marks coincident in the pupil. The distances can then be measured between the marks.

The paraxial radius of curvature is then given by the sum of three measurements:

$$R_v = D1 + D2 + D3$$

Where D1 = the distance from the mirror to the mark on fold flat 3.

D2 = the distance between the marks on fold flat 3 and fold flat 2.

D3 = the distance between the mark on fold flat 2 and the center of fold flat 1.

D1 is measured with a calibrated tape measure traceable to NIST that measures the distance between the mark on fold flat 3 and the edge of the mirror at the center hole. D2 and D3 are measured with inside micrometers having special plastic radiused tips that define the distances (like telescoping gages) that are subsequently measured with calipers. Using these methods we estimate our error in the radius measurement to ± 2mm.

Because the null lens is designed for a mirror having a particular radius of curvature there will be a conic error in the mirror if the radius differs from the design radius. The magnitude of the error is given by:

$$\Delta R/R = \Delta K/K.$$

From this, a radius error of 5 mm will cause a conic error of .0007 in the parabolic mirror.

4.2. Procedure.

1. Check that the paraxial focus of the null lens is in sharp focus on the surface of fold flat 1. If it is not the hologram must be reinserted and the paraxial focus position redefined.

2. Make sure that the calibrated tape is secured with a safety line before using.

3. Viewing the fringes in the monitor mark with a Sharpie a small point (3 mm) on fold flat 3 that coincides in the pupil to a point near the center hole.

4. Make another mark on fold flat 2 that coincides in the pupil to the mark made on fold flat 3.

5. Lower the calibrated tape to a person near the mirror.

6. Holding the end of the tape at the mark on fold flat 3 have the person measure the distance to the polished surface at the edge of the center hole. Record this number in the notebook as D1.

7. Using inside micrometers fixed with the plastic radiused tips measure the distance between the marks on fold flat 3 and fold flat 2.

8. Use calipers to measure the length of the micrometer at the contact points the flats made with the plastic tips. Record this distance in the notebook as D2.

9. Using the inside micrometers again measure the distance between the mark on fold flat 2 and the center of fold flat 1.

10. Use calipers to measure the length of the micrometer at the contact points the flats made with the plastic tips. Record this distance in the notebook as D3.

11. Sum the distances D1 + D2 + D3 to give the paraxial radius of curvature.